Available online at www.sciencedirect.com
ScienceDirect
Catalysis Today 133–135 (2008) 594–599
CATALYSIS TODAY
www.elsevier.com/locate/cattod

Use of TiO_2/Cr-MCM-41 molecular sieve irradiated with visible light for the degradation of thiophene in the gas phase

Fabielle C. Marques *, Maria Cristina Canela, Alexandre M. Stumbo

Laboratório de Ciências Químicas (LCQUI), Universidade Estadual do Norte Fluminense Darcy Ribeiro, Av. Alberto Lamego, 2000 Campos dos Goytacazes-RJ, CEP 28013-602, Brazil

Abstract

Photocatalytic processes using TiO_2 and UV radiation to eliminate pollutants are not yet suitable for industrial facilities due to their high consumption of energy. Transition metals incorporated onto mesoporous MCM-41 molecular sieves impregnated with TiO_2 constitute an alternative that allows the use of solar light. In this study, Cr-substituted MCM-41 were synthesized (Si/Cr = 100, 50 and ∞) and impregnated with TiO_2 (10 and 20 wt.%). Raman results showed the formation of anatase. Electronic spectroscopy and EPR exposed the formation of trivalent chromium after impregnation with TiO_2, which is related to a Cr–TiO_2 interaction. The synthesized photocatalysts, as well as TiO_2 P25, were tested in the degradation of thiophene in gaseous phase. A test with UV lamp showed 100% of conversion for 20%TiO_2/Cr-MCM-41(100) and exceeded the activity of TiO_2 P25, probably due to the higher dispersion of TiO_2 on the surface of the molecular sieve. During tests using visible light and 20%TiO_2/Cr-MCM-41(50) higher conversions than those of 20%TiO_2/Cr-MCM-41(100) and TiO_2 P25 were observed. These results indicate that chromium concentration is a key factor influencing the photocatalytic activity under visible light.

Keywords: Cr-MCM-41; Photocatalysis; Gas phase; TiO_2; Visible light

1. Introduction

After the discovery of TiO_2 electrode photosensibilization for hydrogen generation from the electrolysis of molecular H_2O by Fujishima and Honda [1], heterogeneous photocatalysis using semiconductors has proven to be a promising technology for environmental decontamination. Most of the environmental research involving heterogeneous photocatalysis uses anatase (TiO_2) nanoparticles because of their low toxicity, insolubility in water, chemical stability and photocatalytic activity for mineralization of pollutants in water and air under UV irradiation (wavelengths below 387 nm) [2–4]. When TiO_2 is excited with photons of energy higher than its band gap (E_{gap} = 3.2 eV), electrons (e^-) are promoted from the valence band to the conduction band, creating electronic vacancies or "holes" (h^+) at the valence band edge. The e^-/h^+ pair can promote redox reactions with species adsorbed onto the catalyst. However, only 3–5% of the solar spectrum is in the UV range. Therefore, the cost of installing and operating a large industrial facility would be too high due to the large consumption of energy to artificially produce UV radiation. As a result, recent research efforts have been aimed at producing materials capable of absorbing visible light to develop environmentally clean technologies using solar light as an inexpensive and renewable energy source.

Recently, mesoporous M41S molecular sieves modified by the incorporation of transition metals have been tested in heterogeneous photocatalysis. MCM-41 is the most appealing member from the M41S family because it has a hexagonal array of uniform pores with adjustable diameter (15–100 Å) and exhibits a high surface area (typically $>1000\ m^2\ g^{-1}$) [5]. These characteristics are promising for photocatalysis because they allow for a good dispersion of the active phase as well as easy access to active sites in the pores. In addition, the isomorphic incorporation of transition metals into the structure of MCM-41 can produce catalysts that are active under visible light [6]. Moreover, a previous work demonstrated a good synergy between TiO_2 and Cr-MCM-41 in the destruction of organic pollutants in aqueous phase under visible light [7].

The removal of toxic organic compounds in the gas phase using photocatalytic oxidation has attracted interest in recent

* Corresponding author.
E-mail address: castelan@uenf.br (F.C. Marques).

0920-5861/$ – see front matter © 2008 Published by Elsevier B.V.
doi:10.1016/j.cattod.2007.11.047

years because this technology has advantages when compared to conventional techniques [8–11]. However, the photocatalytic destruction of some compounds can generate products that poison the catalyst and diminish its activity throughout the reaction time. As an example, sulfur-containing volatile organic compounds (VOCS), which are environmental contaminants of elevated toxicity and low odor perceptibility thresholds for humans, may produce sulfate ions when they are destroyed, which can block the access to the active sites [8,9].

The main objective of the present work was to verify the potential application of solar energy in the destruction of pollutants in the gas phase. We conducted experiments to estimate the impacts of xTiO$_2$/Cr-MCM-41 molecular sieves (x = 10 and 20 wt.% and Si/Cr = 100 or 50) in the degradation of sulfurous pollutants in gaseous phase under visible irradiation. The photocatalysts were synthesized and characterized and their activity was evaluated using thiophene (C_4H_4S) as the model compound.

2. Experimental

2.1. Synthesis of the photocatalysts

Cr-MCM-41 molecular sieves with Si/Cr atomic ratios of 100 and 50 were prepared using a hydrothermal method adapted from Blasco et al. [12]. Tetraethylorthosilicate (TEOS; Fluka, 99%) and $CrCl_3{\cdot}6H_2O$ (Vetec, 97%) were used as sources of silicon and chromium, respectively. Initially, $CrCl_3{\cdot}6H_2O$ was added to a *N*-cetyl-*N*,*N*,*N*-trimethylammonium chloride solution (CTACl; Aldrich, 25 wt.%) under stirring. After 30 min, tetramethylammonium hydroxide solution (TMAOH; Fluka, 25 wt.%) was added drop wise under stirring. Finally, the tetraethylorthosilicate was introduced into the mixture and magnetically stirred for 1.5 h. The molar compositions of the reaction mixtures were: 1 SiO_2:0.40 CTACl:0.26 TMAOH:25 H_2O:x Cr_2O_3, (x = 0, 0.005 or 0.010). The final mixture was transferred into a steel autoclave recovered internally with Teflon® and treated under autogenous pressure without stirring at 135 °C for 14 h. The pH of the mixtures, measured before and after the reaction, varied between 11 and 12. Finally, the resulting solids were filtered, washed with distilled water until pH 7 was reached and dried in an oven at 90 °C for 12 h. The template was removed by calcination at 540 °C for 1 h (temperature increase of 2 °C min^{-1}) under flow of N_2 followed by 5 h under airflow at the same temperature.

The resulting materials were impregnated with 10 and 20 wt.% of TiO_2 by hydrolysis of titanium (IV) isopropoxide (Aldrich, 97%). The molecular sieve (typically 1.0 g) was dispersed with 80 mL of isopropyl alcohol (Synth, p.a.) and the proper amount of Ti(Oip)$_4$ was added to achieve the desired TiO_2 loading. The suspension was stirred at ambient temperature for 1 h and then the solvent was evaporated under heating at 50 °C. The samples were dried in an oven for 1 h at 90 °C and calcined at 450 °C under airflow for 4 h. The catalysts obtained were identified as: 10 or 20% TiO_2/Cr-MCM-41(50) and 10 or 20% TiO_2/Cr-MCM-41(100), where the percentage is the TiO_2 content (wt.%) and the number between parenthesis is the Si/Cr ratio.

2.2. Surface area, pore size and pore volume

Surface areas and pore size distribution studies were conducted by N_2 physisorption at 77 K using a Quantachrome Autosorb 1C. All samples were degassed for 1 h at 300 °C under vacuum before analysis. Surface areas and pore size distributions were determined using BET (P/P_0 = 0.05–0.30) and BJH methods, respectively, both through Autosorb for Windows® software, version 1.24.

2.3. Raman spectroscopy with Fourier transform

Raman spectra were recorded with a Nicolet Fourier Transform Spectrometer, model 950 FT-RAMAN, equipped with a Ge detector and a Nd:YAG (1064 nm) laser source (100–200 mW). Spectra averaged 128 scans, with a resolution of 4 cm^{-1}.

2.4. Diffuse reflectance spectroscopy (DRS)-UV–Vis

The catalysts were characterized by DRS using a Varian spectrophotometer equipped with a ISR1200 integrating sphere attachment. Diffuse reflectance spectra were recorded in the range of 200–800 nm, using $BaSO_4$ as a reference.

2.5. Electron paramagnetic resonance (EPR)

EPR spectra were recorded at 77 K using quartz tubes. A Bruker Spectrometer (model ESP 300E) was used operating at a frequency of 9.7 GHz (X-Band) with a modulation frequency of 100 kHz and a modulation amplitude of 2.024 G and 20 mW of microwave power.

2.6. Photocatalytic test

Photocatalytic tests were carried out using a steel tubular photo-reactor. A lamp (black light or visible light) was placed along the central axis of the reactor. The middle section was narrower, creating a thin annular space between the lamp and the outer wall, where approximately 200 mg of catalyst were placed. Void spaces in the reactor were filled with glass beads. A schematic representation of the photocatalytic degradation system is shown in Fig. 1. The black light lamp (4 W Luxor® BLB) has its maximum intensity at 365 nm and the visible light lamp (4 W Ning®) had an emission band of 400–600 nm.

Synthetic air ($O_2 = 20 \pm 0.5\%$ and $H_2O < 3$ ppm-White Martins) was used as carrier gas. Part of the flow passed through a saturator containing liquid thiophene (Fluka, ≥98.0%) immersed in a bath kept at 10 °C. The contaminated gas was mixed with a stream of pure air to adjust the final thiophene concentration to approximately 500 ppmv and the total flow rate to 115 mL min^{-1}.

Conversion rates were monitored using a Shimadzu GC-17B gas chromatograph equipped with a DB-1 (30 m × 0.25 mm

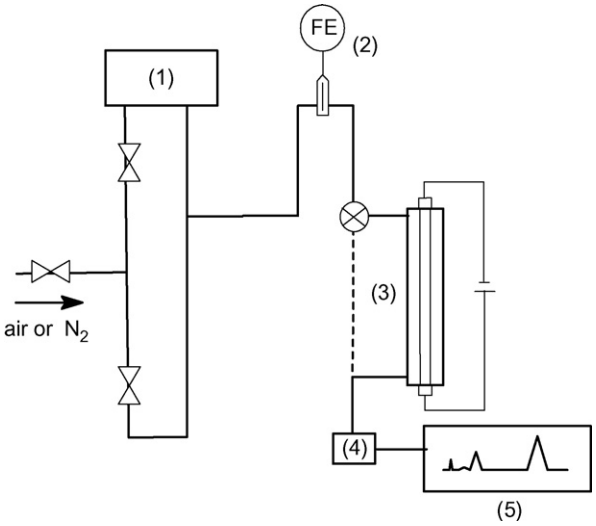

Fig. 1. Schematic representation of photocatalytic degradation system: (1) thermostatized saturator containing liquid thiophene; (2) flow meter; (3) photoreactor; (4) thermostatized 6-way injection valve; (5) GC-FID on-line.

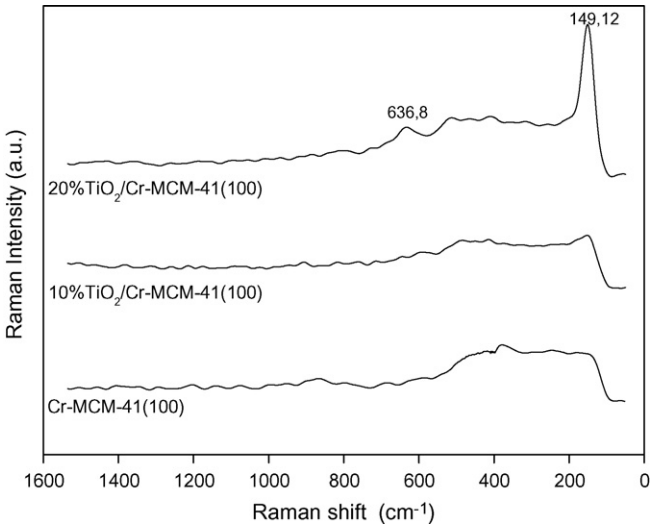

Fig. 2. Raman spectra of Cr-MCM-41(100) molecular sieves before and after TiO_2 impregnation.

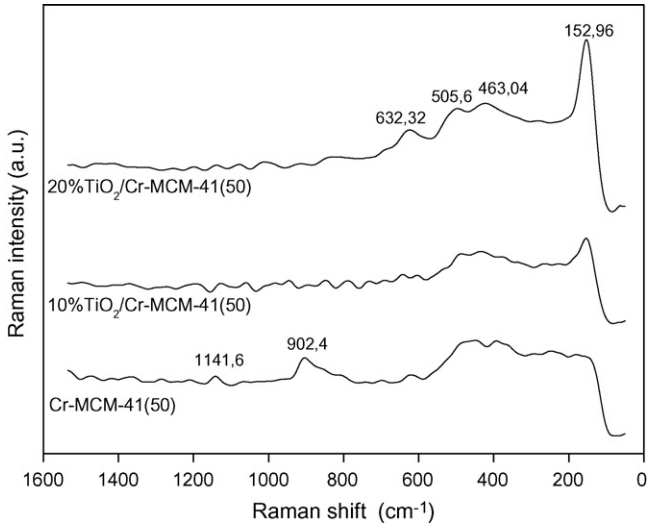

Fig. 3. Raman spectra of Cr-MCM-41(50) molecular sieves before and after TiO_2 impregnation.

$\times$ 0.25 μm, J&W) fused silica capillary column and a flame ionization detector. Sampling was done on-line by an automated 6-way valve (Valco) at programmed intervals of 20 min.

3. Results and discussion

3.1. Surface area, pore size and pore volume

The N_2 physisorption isotherms of the synthesized samples are of type IV, according to IUPAC classification, typical of mesoporous structures [13]. Isotherm profiles were not modified by TiO_2 impregnation. Isotherms of Cr-MCM-41(100), 10%TiO_2/Cr-MCM-41(100) and 20%TiO_2/Cr-MCM-41(100) present H3 hysteresis loops, associated to partially disordered structures, due to the formation of some pores larger than the majority of the mesopores of the molecular sieve [13]. Indeed, BJH calculations showed two maxima in the pore size distributions, around 46 Å (minor part) and 23 Å (see Table 1). This bimodal distribution has already been reported for Cr-MCM-41 with Cr/Si = 0.02(Si/Cr = 50) [14]. The formation of larger pores in molecular sieves containing chromium was associated with the formation of defects (or distortions) in the structure. During and after the hydrothermal synthesis, Cr was present as Cr^{3+} in pseudo-octahedral coordination to oxygen. Upon calcination, this Cr^{3+} is oxidized to Cr^{6+}, mainly as monochromate/polychromate species, assuming a tetrahedral coordination. However, only two out of the four bonds formed with oxygen atoms within the framework. The two other bonds formed with oxygen atoms located outside the framework, thus creating distortions [14]. This observation was supported by the higher pore volume presented by the Cr-MCM-41(100) molecular sieve when compared to the sample without Cr (Si-MCM-41).

Table 1
Results of textural characterization

Catalyst	BET (m^2/g)	Pore size (Å)	Pore volume (cm^3/g)
Cr-MCM-41(100)	828	29/46	0.83
20%TiO_2/Cr-MCM-41(100)	724	23/46	0.63
Cr-MCM-41(50)	771	29	0.77
20%TiO_2/Cr-MCM-41(50)	694	23	0.59
Si-MCM-41	1412	23	0.79
TiO_2 (Degussa-P25)	51.5	n.a[a]	n.a[a]

[a] n.a: not applied.

3.2. Raman spectroscopy with Fourier transform

The Raman spectra from calcined samples before and after impregnation with TiO_2 are represented in Figs. 2 and 3. The spectrum of the sample with higher Si/Cr ratio (Fig. 2) is featureless before TiO_2 impregnation, indicating the absence of

polychromate species [14]. The spectra obtained after TiO_2 impregnation present a band at 149 cm^{-1} whose intensity increases with titanium content. The spectrum of 20%TiO_2/Cr-MCM-41(100) shows another band at 636 cm^{-1}. Both bands have been attributed to Ti–O groups in anatase particles [15].

The sample with lower Si/Cr ratio (Fig. 3) shows two bands, at 1141 and 902 cm^{-1}, before TiO_2 impregnation. These bands, which are not present in the Cr-MCM-41(100) spectrum (Fig. 2), are associated with vibrations of Cr–O bonds from polychromates and hydrated chromates, respectively [14]. After impregnation, bands from anatase appear and polychromates and chromates bands decrease (or disappear), probably due to the interaction with the superficial TiO_2. This observation suggests that titanium is in close contact with chromium in these molecular sieves, increasing the possibility of charge transfer between the two species during the photocatalytic process.

3.3. Diffuse reflectance spectroscopy–UV–Vis

Fig. 4 shows UV–Vis spectra of Cr-MCM-41 impregnated with 20 wt.% TiO_2. The chromium-containing materials show absorption beginning at approximately 600 nm, whereas the samples without chromium absorb only in the UV range. The presence of the heteroatom reduced the bandgap energy (the separation between valence and conduction bands in the semiconductor) from the 3.2 eV found for pure TiO_2 to ≈2.0 eV. These results show that the synthesized materials have a great potential as photocatalysts able to use solar light.

DRS spectrum of calcined Cr-MCM-41(100) has two intense bands at 275 and 390 nm, attributed to O(2p) → $Cr^{6+}(3d^0)$ charge transfer of chromate (CrO_4^{2-}) species, indicating that chromium is oxidized to Cr(VI) during calcination. These results are in accordance to those of Hogan [17] and McDaniel [18]. After impregnation of TiO_2, those maxima corresponding to Cr^{6+} overlap, resulting in a virtually unique absorption. A band at ≈350 nm confirmed the formation

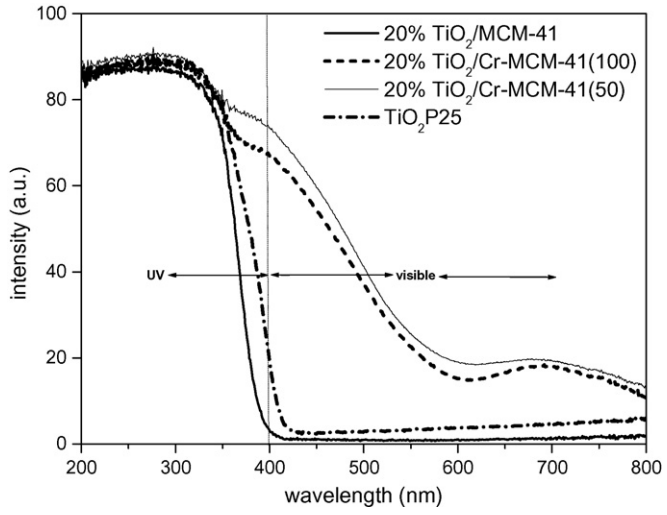

Fig. 4. DRS-UV–Vis spectra of the molecular sieves impregnated with 20 wt.% TiO_2.

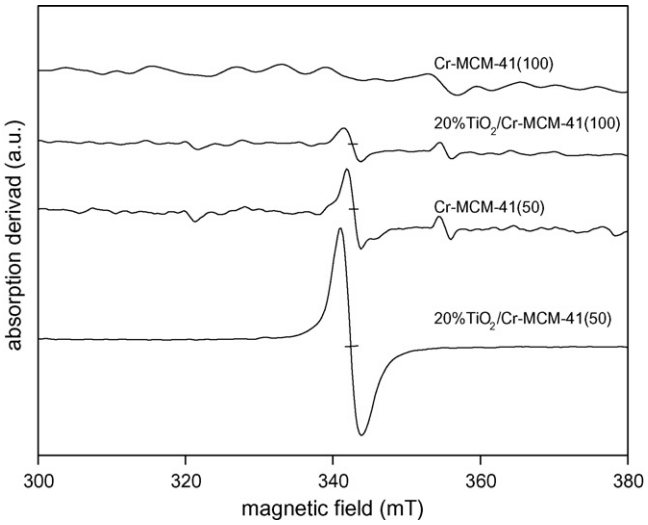

Fig. 5. EPR spectra of calcined samples before and after TiO_2 impregnation.

of anatase TiO_2 [19]. The coincidence of bands between TiO_2 and chromate species shows that the absorption in the range of 370–500 nm is related to a heterojunction of titania and chromium. The spectra of chromium-containing samples showed an absorption band around 700 nm in the red region of the electromagnetic spectrum assigned to d–d transitions described as $^4A_{2g}(F) \rightarrow {}^4T_{2g}(F)$ from Cr^{3+} in octahedral coordination [16].

3.4. Electron paramagnetic resonance (EPR)

EPR results of calcined samples are represented in Fig. 5. Cr-MCM-41(100) is the only sample that does not absorb the microwaves. Chromium has three oxidation states with unpaired spin: Cr^{3+} ($3d^3$, $^4F_{3/2}$), Cr^{5+} ($3d^1$, $^2D_{3/2}$) and Cr^{1+} ($3d^5$, $^6S_{5/2}$), all active in EPR. Cr^{3+} is the most stable paramagnetic species. Chromium in Cr-MCM-41 will preferentially assume octahedral coordination instead of the tetrahedral coordination required to the isomorphic substitution of Si on the silicate. This statement is based on the higher value of the crystal field stabilization energy of the octahedral Cr^{3+} (224 kJ mol^{-1}) when it is compared to the tetrahedral (67 kJ mol^{-1}) [20].

As discussed previously, during calcination the Cr^{3+} in Cr-MCM-41 was oxidized to diamagnetic Cr^{6+} and assumed a tetrahedral coordination that formed bonds with two oxygen atoms outside the framework. In Fig. 5, the absence of absorption in Cr-MCM-41(100) was observed while 20%TiO_2/Cr-MCM-41(100), Cr-MCM-41(50) and 20%TiO_2/Cr-MCM-41(50) showed an absorption at approximately 350 mT, corresponding to a constant $g \approx 1.98$. This signal can be attributed to the formation of Cr^{3+} in octahedral coordination [21], indicating an extensive reduction of Cr^{6+} after TiO_2 impregnation. It is well known that Cr^{6+} and Cr^{5+} are good electron acceptors as they can be easily reduced [20].

Fig. 6 presents a scheme of the Cr-MCM-41 structure based on the spectroscopy studies, before and after TiO_2 impregnation. It is observed that the formation of TiO_2 occurs via reduction of the Cr^{6+} in the structure of the molecular sieve to Cr^{3+}.

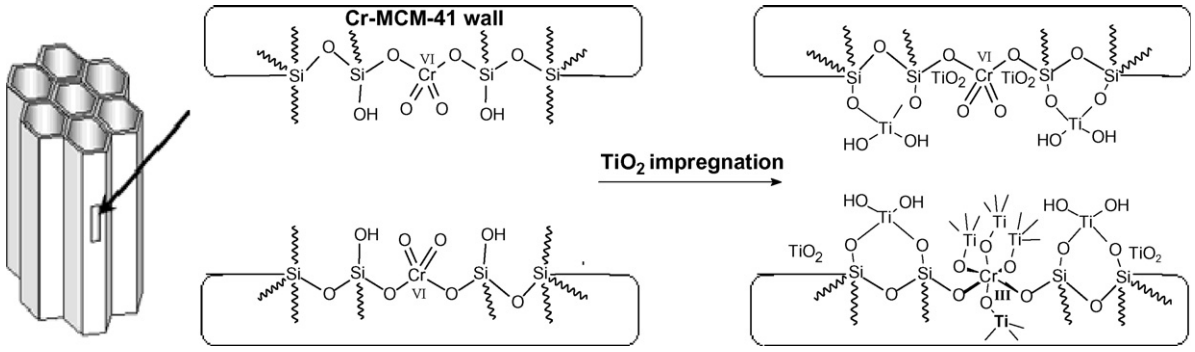

Fig. 6. Mechanism proposed for the reduction of Cr after TiO_2 impregnation.

3.5. Photocatalytic activity using UV light

In this study, thiophene photodegradation tests were effectuated using an UV lamp. Fig. 7 compares the activities of the synthesized materials (Si/Cr = 100, 50 and ∞, impregnated with 20 wt.% of TiO_2) and TiO_2 P25 (Degussa). After 80 min of irradiation, total photodegradation of the thiophene was observed when using 20%TiO_2/Cr-MCM-41(100). Under the same conditions, TiO_2 P25 destroyed approximately only 60% of the contaminant. The superior photocatalytic activity of the molecular sieve over the traditional catalyst can be explained by its higher surface area that lead to a better dispersion of the impregnated TiO_2 and an increase in the number of accessible active sites. The results have also shown that the molecular sieve with lower Si/Cr ratio has the lowest photodegradation activity. The chromium content should not directly influence the conversion of thiophene since TiO_2 should be the only species responsible for the activity under UV light. However, there is probably a direct influence of the chromium on the dispersion of TiO_2 on the Cr-MCM-41 surface, suggesting that there should be an ideal chromium concentration.

Fig. 8 shows a deactivation test performed with the most active sample. The photocatalytic activity of 20%TiO_2/Cr-MCM-41(100) goes down after 5 h of irradiation. Deactivation in the presence of VOCS has been described in the literatures [22,23], but the mechanism is not well established. Some studies concluded that sulfate ions formed during the photooxidation were reversibly adsorbed onto the catalyst surface, temporarily blocking the active sites [22]. In this work, FTIR analysis of the catalysts after photocatalytic tests did not show the formation of sulfate ions or other non-volatile species. Peral and Ollis [23] observed a 10% conversion of dimethyl sulfide using TiO_2/UV and no appreciable deposition of sulfur or sulfate onto TiO_2. According to the authors, either S is removed continuously as SO_2 or SO_3, or the mercaptan is only partially converted and the partial oxidation gaseous products still contain the S atom.

3.6. Photocatalytic activity using visible light

Fig. 9 presents the results of the photocatalytic tests for molecular sieves with Si/Cr = 100, 50 and ∞ irradiated with visible light. The test using 20%TiO_2/Cr-MCM-41(50) showed high efficiency, reaching degradation yields of 40%, after 140 min of irradiation. Under the same conditions, TiO_2 P25

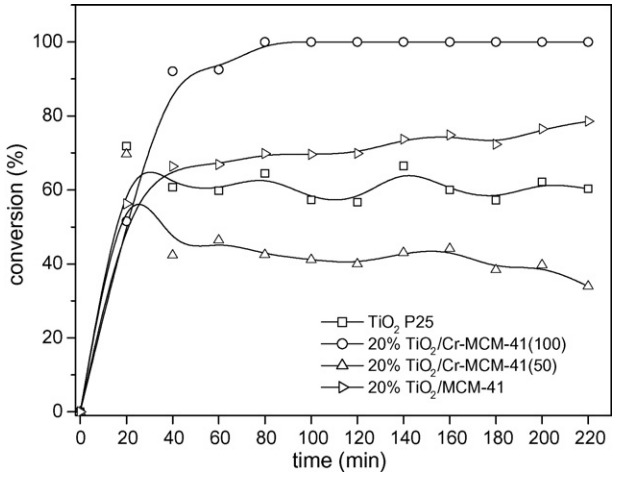

Fig. 7. Photodegradation of thiophene on different catalysts irradiated with UV light. Conditions: C_0 = 500 ppmv; catalyst = 200 mg; 115 mL $min^{-1}$of synthetic air (O_2 = 20 ± 0.5% and H_2O < 3 ppm).

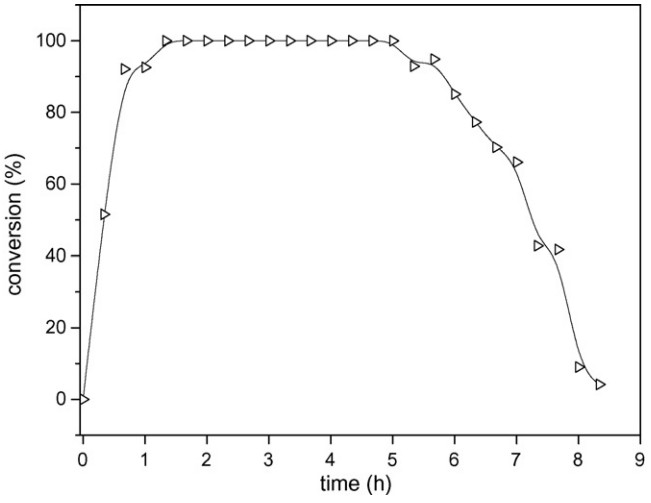

Fig. 8. Deactivation of the photocatalyst 20%TiO_2/Cr-MCM-41(100). Conditions: UV light; C_0 = 500 ppmv; catalyst = 230 mg; 115 mL min^{-1} of synthetic air (O_2 = 20 ± 0.5% and H_2O < 3 ppm).

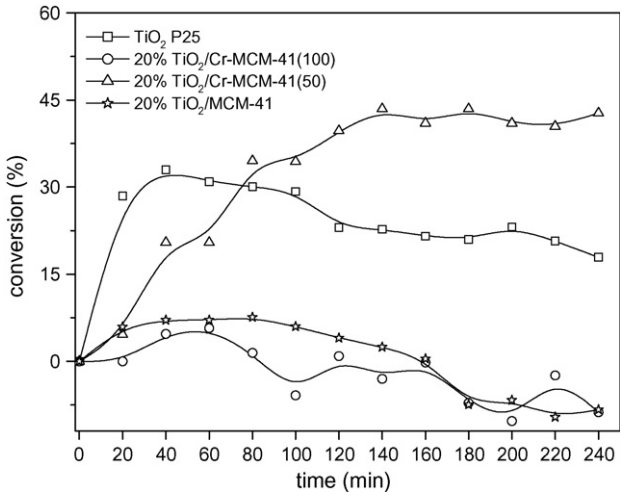

Fig. 9. Photodegradation of thiophene on different catalysts irradiated with visible light. Conditions: $C_0 = 500$ ppmv; catalyst = 200 mg; 115 mL min^{-1} of synthetic air ($O_2 = 20 \pm 0.5\%$ and $H_2O < 3$ ppm).

converted only 20% of the thiophene. These results show the potentiality of the synthesized materials for pollutants photooxidation using solar light.

The formation of electron/hole pairs in 20%TiO_2/Cr-MCM-41(50) was suggested to occur via Cr^{6+} through an electronic transition promoted by visible light: $Cr^{6+} = O^{2-} \rightarrow (Cr^{5+}–O^{-})^{*}$. Cr^{5+} species can possibly donate an electron to the neighboring TiO_2. In the decay process, O^{-} of the photoexcited chromate species can withdraw electrons from the TiO_2 particles, leaving an oxidant hole in the valence band [6]. The molecular sieve with higher Si/Cr ratio showed lower activity indicating that chromium content is an important parameter to determine the activity level under visible light irradiation.

All synthesized materials presented a gradual deactivation during the tests, attributed to a progressive reduction of Cr^{6+} to Cr^{3+} and Cr^{2+} by accumulated electrons on the surface of the catalyst [6].

4. Conclusions

Different characterization techniques indicated that part of the chromium in the photocatalyst 20%TiO_2/Cr-MCM-41(100) is in the form of monochromate species that create defects in the framework of the molecular sieve. This distortion is caused by the difficulty of chromium to assume tetrahedral coordination during the synthesis and result in a bimodal distribution of pore sizes. The impregnation of TiO_2 decreased the bandgap energy of the semiconductor due to the Cr–O–Ti junction.

A test using UV light verified the total photooxidation of thiophene using the 20%TiO_2/Cr-MCM-41(100) catalyst. The molecular sieve with lower Si/Cr ratio had the lowest conversion. The degradation yields were higher than those of pure TiO_2 and were attributed to a better dispersion of TiO_2 on the surface of the molecular sieve that result from the high surface area of this kind of support.

Photocatalytic tests using visible light showed that 20%TiO_2/Cr-MCM-41(50) converted 40% of the thiophene, whereas TiO_2 P25 converted only 20%. The photocatalyst with higher Si/Cr ratio showed lower conversion. This indicates that when visible light is used Cr^{6+} content is an important parameter determining the activity of the photocatalyst.

M41S molecular sieves, when modified by the incorporation of transition metals and the impregnation of TiO_2, are an alternative that takes advantage of solar light, an inexpensive and renewable source of energy, in the photodegradation of pollutants in gaseous phase.

Acknowledgements

The authors acknowledge the financial support from UENF-FAPERJ (grants) and Conselho Nacional de Desenvolvimento Cientifico e Tecnológico (CNPq) (CNPq proc. 471.238/03-1 and PADCT-RIO 62000803-2/03). We also acknowledge the Department of Chemistry (PUC-Rio) for Raman analysis, LABRPE/DQ/UFPR for EPR results and IQ-Unicamp for DRS-UV–Vis analysis.

References

[1] K. Honda, A. Fujishima, Nature 238 (1972) 37.
[2] R.W. Matthews, Water Res. 24 (1990) 653.
[3] M.A. Fox, M.T. Dulay, Chem. Rev. 93 (1993) 341.
[4] M.R. Hoffmann, S.T. Martin, W. Chio, D.W. Bahnemann, Chem. Rev. 95 (1995) 69.
[5] C.T. Kresge, M.E. Leonowicz, W.J. Roth, J.C. Vartuli, J.S. Beck, Nature 359 (1992) 710.
[6] L. Davydov, E.P. Reddy, P. France, P.G. Smirniotis, J. Catal. 203 (2001) 157.
[7] B. Sun, E.P. Reddy, P.G. Smirniotis, J. Catal. 237 (2006) 314.
[8] A.V. Vorontsov, E.V. Savinov, L. Davydov, P.G. Smirniotis, Appl. Catal. B: Environ. 32 (2001) 11.
[9] M.C. Canela, R.M. Alberici, R.C.R. Sofia, M.N. Eberlim, W.F. Jardim, Environ. Sci. Technol. 33 (1999) 2788.
[10] R.M. Alberici, W.F. Jardim, Appl. Catal. B: Environ. 335 (1997) 1.
[11] S. Chiron, A. Fernandez-Alba, A. Rodriguez, E. Garcia-Calvo, Water Res. 34 (2000) 366.
[12] T. Blasco, A. Corma, M.T. Navaro, J.P. Pariente, J. Catal. 156 (1995) 65.
[13] K.S.W. Sing, D.H. Everett, R. Haul, Pure Appl. Chem. 57 (1985) 603.
[14] M.B. Weckhuysen, I.E. Wachs, R.A. Schoonheydt, Chem. Rev. 96 (1996) 3327.
[15] G.T. Went, S.T. Oyama, A.T. Bell, J. Phys. Chem. 94 (1990) 4240.
[16] Z. Zhu, Z. Chang, L. Kevan, J. Phys. Chem. B 103 (1999) 2680.
[17] J.P. Hogan, J. Polym. Sci. 8 (1970) 2637.
[18] M.P. McDaniel, J. Catal. 76 (1982) 37.
[19] M.A. Camblor, A. Corma, A.J. Martinez, Chem. Commun. 8 (1992) 589.
[20] B.M. Weckhuysen, R.A. Schoonheydt, Stud. Surf. Sci. Catal. 84 (1994) 965.
[21] J.S.T. Mambrim, H.O. Pastore, C.U. Davanzo, J.S. Vichi, O. Nakamura, H. Vargas, Chem. Mater. 5 (1993) 166.
[22] M.C. Canela, R.M. Alberici, W.F. Jardim, J. Photochem. Photobiol. A 112 (1997) 73.
[23] J. Peral, D.F. Ollis, J. Mol. Catal. A: Chem. 115 (1997) 347.